SOLAR THERMAL COLLECTOR'S DEGRADATION – INFLUENCE OF CORROSIVITY INSIDE AND OUTSIDE THE COLLECTORS

M.J. Carvalho[1], S. Páscoa[1], N. Mexa[1], R. Gonçalves[1], J. Correia[1], A. Gano[1], T. Diamantino[1]

[1] LNEG - Laboratório Nacional de Energia e Geologia I.P., Lisboa (Portugal)

Abstract

Influence of atmospheric corrosivity on solar thermal collector's degradation was studied by exposure of flat plate collectors to two different corrosivity environments, one urban Outdoor Exposure Testing (OET) site with medium corrosivity (C2-C3) and a very high/extreme corrosivity (industrial and marine) (C5-CX) atmosphere highly polluted and simultaneously with highly airborne salinity. Results of thermal performance measurements after two years of exposure in the two OET sites are presented, as well as the evaluation of the corrosion rate inside the collectors, with zinc as reference material, atmospheric contaminants, temperature and relative humidity. For the measurement of temperature and relative humidity inside the collectors, in house produced data acquisition system and sensors were used and are shortly described. Collectors were dismantled and optical properties of the absorbers were measured.

Keywords: *Solar thermal collectors, atmospheric corrosivity, thermal performance degradation*

1. Introduction

Solar thermal collectors (STC) have to withstand stress conditions like high temperatures, high humidity, ultraviolet irradiance or wind and snow loads depending on the geographic location. Literature points out to dependence on other influences like prevailing wind conditions, contaminants like chlorides, SO_2 and NO_x, global solar irradiation, wetness time and precipitation (Köhl et al., 2004; Slamova et al., 2016).

Although for certification of solar thermal collector (e.g. Solar Keymark, SRCC), the testing standards applied, namely ISO 9806:2013, consider a set of tests which address testing of collector resistance to most common adverse conditions when collectors are in use, these tests do not address long term collector durability.

In order to better know how different environmental conditions influence STC, as well as collector components, two OET (Outdoor Exposure Testing) sites were used to expose collectors and collector components. The two OET sites represent an urban climate (Lumiar-Lisboa) and a maritime climate with industrial influence (Sines) (Diamantino et al., 2017). The results of collector exposure will be presented in this work for the two OET sites after two years of exposure. Corrosion rate for zinc, atmospheric contaminants, temperature and relative humidity inside de collectors are also presented. Collectors were dismantled and absorber optical properties measured.

2. Materials and methods

2.1. Exposure of STC at OET sites

STC studied were Flat Plate Collectors with tempered glass cover, commercially available. Their main characteristics are described in Table 1.

For each collector model, two samples were exposed in each OET sites (see Figure 1). Thermal performance was measured before exposure for each collector model. For three of the models, zinc standard specimens were installed inside one of the collector samples. After two years exposure, thermal performance was measured. Preliminary results for one of the OET sites were presented in (Carvalho et al., 2016). Summary of all thermal performance results are presented in this work, in section 3.2.

doi:10.18086/swc.2017.19.02 Available at http://proceedings.ises.org

Tab. 1: Main collector characteristics

Collector reference	Type of collector
A *	Aluminum absorber surface with PVD coating (Mirotherm ®); Aluminum box
C *	Aluminum absorber surface with PVD coating (Eta plus ®); Aluminum box.
D *	Copper absorber surface with selective paint coating (SUNCOLOR TS S Black); Stainless steel box.
*1 replicate with zinc standard specimens	

Fig. 1: Installation of collectors in OET sites - Urban (left); Maritime/Industrial (right)

2.2. STC thermal performance evaluation method

Thermal performance tests of solar thermal collectors were performed according to ISO 9806:2013, using quasi-dynamic test method. The comparison is made based on the power curve as defined in ISO 9806:2013 for normal incident irradiance of 1000 W m^{-2} (Direct irradiance = 850 W m^{-2}; Diffuse irradiance = 150 W m^{-2}).

Initial thermal performance was measured only in one collector of each reference. Final results of thermal performance were measured for all collector models exposed. The collectors with installed reference materials were dismantled for inspection and for evaluation of the corrosion rate in zinc samples as well as atmospheric contaminants (chlorides, nitrates and sulphates).

2.3. Optical properties of absorbers

Optical properties of absorbers were also measured. Information on optical properties of absorbers used in each collector exists and will also be presented (initial values) and compared with the performed measurements of the absorber samples extracted from collectors, after two years exposure.

The measured optical properties were solar absorptance (α_s) and thermal emittance (ε_t). The solar absorption (α_s) was measured using a Perkin Elmer's Spectrophotometer Lambda 950 UV/VIS/NIR with a 150 mm integrating sphere.

The thermal emittance (ε_t) was initially determined with a portable emissometer, Devices & Service Company model AE-AD3, which measures a surface emittance at 80 °C of temperature and corrected for a temperature of 100 ºC based on later measurements using a Spectrophotometer Frontier IR/NIR of Perkin Elmer, with integrating sphere.

2.4. Zinc corrosion rate inside STC and atmospheric contaminants evaluation

In each of the collectors referenced in Table 1 with *, five (5) replicates of zinc metal samples were put in the air gap between absorber and glazing (Carvalho, et al, 2016), to evaluate the corrosivity of the microclimate after approximately two years exposure. Zinc samples inside the collectors are equal to the zinc samples placed outdoors to comparatively evaluate the atmospheric corrosivity. The corrosion categories of outdoor exposure test sites were obtained by determination of the corrosivity based on corrosion rate measurement of standard specimens (carbon steel, zinc, copper and aluminum) according to ISO 9223: 2012 and ISO 9226:2012 during

main period of STC exposure.

The atmospheric contaminants present in the solar absorber surfaces, inside the collectors, were also collected by Bresle method (ISO 8502-6, 2006) and analyzed by Ion chromatography. Atmospheric contaminants were analyzed in three different parts of the collectors (1, 2 and 3). In Figure 2 is possible to see the zinc reference materials (5 samples) and where environmental contaminants were collected (1, 2 and 3),

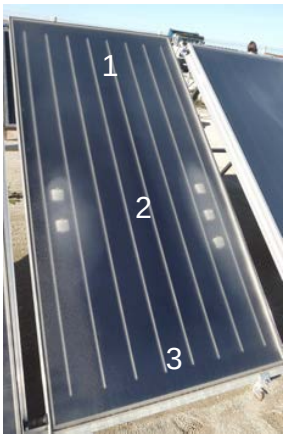

Fig. 2: STC with zinc reference materials and the indication where environmental contaminants were collected after dismantling of collectors

2.5. Measurement of STC inside temperature and relative humidity

Aiming STC's internal temperature and relative humidity measurement and analysis over a predefined period under real working conditions, a custom real-time monitoring and data-logging programmable smart data acquisition system was developed and prototypes were implemented for 'in-situ' data collection in the two OET sites.

Due to the internal ambient working STC conditions, with peak temperatures exceeding 120 ºC, most commercial relative humidity (RH) measuring and logging equipment do not comply with these specifications, mainly due to temperature restrictions of most of the relative humidity electronic sensors available in the market.

The developed system has the following specifications:

- two custom sensor probes for insertion in two STC's, each with one resistive thermal platinum sensor (Pt_{100}) and one high temperature capacitive relative humidity sensor (see Figure 3a):
  - temperature measuring range: -10 to 150 ºC with ±0.1 ºC resolution;
  - relative humidity range: 0 to 100% (non condensing) with ±5 % resolution, with [-10 ºC, +150 ºC] working temperature range;
- programmable sampling periods sets, ranging from 1 sample/min (1440 Samples/Day), as maximum sample rate, to 1 sample/ 4 Hours (6 Samples/Day) as minimum sampling rate;
- system power autonomy of at least one year, for a full set of variables data logging with a sampling period greater than 15 min;
- local data logging of the acquired data using internal non-volatile flash memory;
- data communication with an external computer for system configuration and data gathering using a standard USB2.0 interface;

This custom smart data acquisition and processing unit (see Figure 3b) enables the simultaneous monitoring and data logging of two separate, but adjacent, solar thermal collectors, being its hardware based on a low power, high performance 16-bit microcontroller. This custom unit includes extra functionalities for increased flexibility in signal acquisition, local data processing and external data communication, without compromising system's energy autonomy. Special attention was paid to the system's power consumption in order to keep the intended system's autonomy, being used ultra-low power electronic circuits whenever possible.

The system was developed having in mind an high configurability and flexibility in data acquisition and logging, in order to perform internally all data processing for an 'all digital' information output, along with optimized algorithms to minimize the system's power consumption when active.

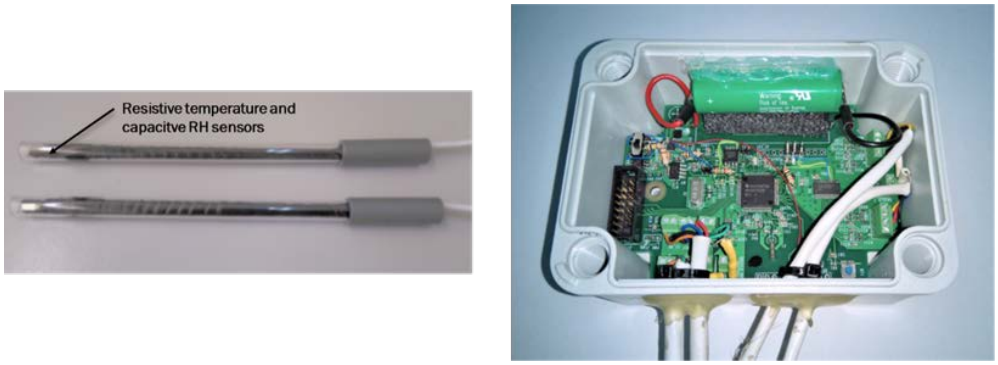

Fig. 3: Collector's internal sensor probes with resistive platinum Pt100 temperature sensor and a high temperature capacitive sensor for relative humidity (Left); b) Custom smart data acquisition and processing unit (right).

A custom user interface software (see Figure 4) was also developed for system's configuration and logged data gathering. The software application runs under Windows environment, allowing an easy system's operation. The logged data can directly be imported into Excel datasheets using a standard text file with CSV format, being each recorded sample stamped with Date/Time information from the system's internal real-time clock, synchronized with the computer's clock when the system is initially configured to start acquisition.

This smart monitoring system is presently being enhanced to include, in the near future, new sensors for other collector's physical environmental variables, like ambient temperature and relative humidity, internal absorber working temperature, UV irradiation, etc,

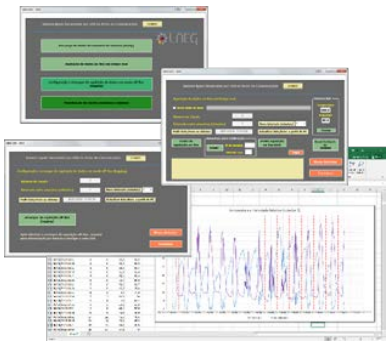

Fig 4. System's user interface for configuration and data gathering

2.6. Scanning Electron Microscopy (SEM) with Energy Dispersive X-ray Spectroscopy (EDS)

The morphology of solar absorber surfaces (after two year of exposure in Sines OET sites) were examined using a Philips Scanning Electron Microscope, Model XL30 FEG with Energy Dispersive X-ray Spectroscopy (EDS) associated. Before observation, the samples were cut in a cut-off machine to a 1.0 cm X 2.0 cm size. After that, for better conduction, samples were gold coated in the Emitech K575X turbo sputter coater, for 5 seconds.

3. Results and Discussion

3.1. OET sites characterisation

The characterization of Sines and Lumiar-Lisboa OET sites is presented in Table 2 with indication of yearly values in terms of main climatic parameters. A more detailed presentation of ambient temperature and global irradiance can be seen in Fig. 5. Table 3 and 4 present the corrosion rates and atmospheric corrosion categories for Sines and Lumiar-Lisboa OET site, respectively.

These results show the different environmental parameters and corrosivities of Sines and Lumiar-Lisboa OET sites. Both have similar temperature and relative humidity mean values, although Sines with slightly higher mean values. The differences lie in atmospheric contaminants (chlorides and sulphur dioxide deposition values) with much higher values in Sines. In terms of corrosivity, Sines has a high corrosivity for aluminum (category C4), very high for steel and zinc (category C5) and extreme for copper category CX. Lumiar-Lisboa with low corrosivity for aluminum and steel (category C2), medium for zinc (category C3) and medium-high for copper (category C3-C4).

Tab. 2: Climate characterization in the two OET sites (2014-2015) (Sines and Lumiar-Lisboa)

Location	Latitude	Longitude	Altitude	Year	Average ambient temperature [°C]	Average relative humidity [%]	Cl^- [mg day^{-1} m^{-2}]	SO_2 [mg day^{-1} m^{-2}]
Sines	37.95°N	-8.88°W	17 m	2014	16.9	78.7	191.8	139.1
				2015	17.9	81.2	89.5	93.4
Lumiar Lisboa	38.77°N	-9.17°W	116 m	2014	16.6	76.9	15.4	10.8
				2015	17.2	77.6	16.9	33.0

Tab. 3: Corrosion rates of carbon steel, copper, zinc and aluminum and corrosion categories measured in Sines OET site

Sines OET site				
Reference materials	**Carbon steel**	**Copper**	**Zinc**	**Aluminum**
Corrosion rate (g m^{-2} y^{-1})* (2014)	1346.01	64.33	59.16	3.98
Corrosion rate (g m^{-2} y^{-1})* (2015)	981.11	52.01	44.08	2.21
Category/corrosivity (Year)	**C5 / Very High (2014)**	**CX / Extreme (2014)**	**C5 / Very High (2014)**	**C4 / High (2014)**
Category/corrosivity (Year)	**C5 / Very High (2015)**	**CX / Extreme (2015)**	**C5 / Very High (2015)**	**C4 / High (2015)**

*corrosion rates expressed in grams per square meter per year

Tab. 4: Corrosion rates of carbon steel, copper, zinc and aluminum and corrosion categories measured in Lumiar-Lisboa OET site

Lumiar-Lisboa OET site				
Reference materials	**Carbon steel**	**Copper**	**Zinc**	**Aluminum**
Corrosion rate (g m^{-2} y^{-1})* (2014)	163.29	11.51	9.85	0.25
Corrosion rate (g m^{-2} y^{-1})* (2015)	194.35	16.76	6.69	0.20
Category/corrosivity (Year)	**C2 / Low (2014)**	**C3 / Medium (2014)**	**C3 / Medium (2014)**	**C2 / Low (2014)**
Category/corrosivity (Year)	**C2 / Low (2015)**	**C4 / High (2015)**	**C3 / Medium (2015)**	**C2 / Low (2015)**

*corrosion rates expressed in grams per square meter per year

In Figure 5 it is represented the frequency distribution of irradiance and ambient temperature of both OET sites (September 2016 to August 2017). Although ambient temperature average values are slightly higher in Sines, Lumiar-Lisboa has higher ambient temperature amplitudes. The irradiance behavior is similar in both OET sites although with higher irradiance values for Sines.

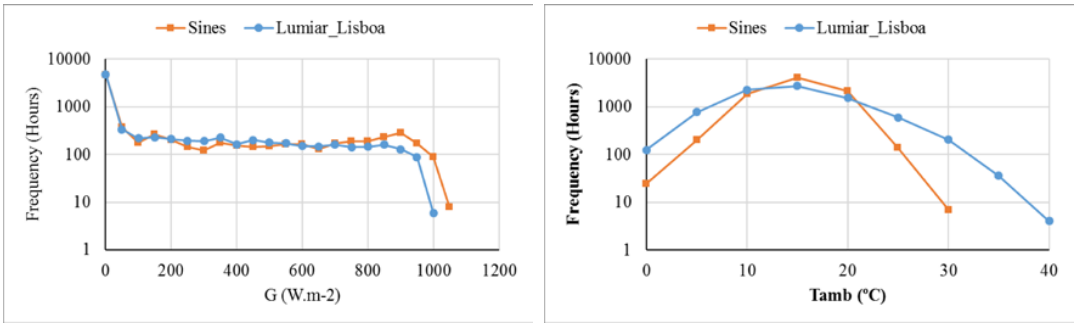

Fig. 5: Irradiance (global) (Left): Ambient temperature (right)

3.2. STC thermal performance and optical properties after approximately two years exposure

In a previous paper (Carvalho, et al, 2016) the thermal performance evaluation for collectors exposed in Sines after one and two years exposure was presented. In this work, only results with two years exposure, both for Sines and Lumiar-Lisboa, are presented. In Table 5 the periods of exposure of these collectors are listed.

Tab: 5 – Exposure dates of STC in Sines and Lumiar-Lisboa OET sites

	Model (Ref.)	Installation date	Uninstallation data	Exposure time (month)
Sines	S_A2 *(**)	11-04-2014	01-06-2016	26
	S_C2 * (**)	09-05-2014	01-06-2016	25
	S_D2 *	11-04-2014	01-06-2016	26
Lumiar-Lisboa	L_A2 * (**)	23-06-2014	11-11-2016	30
	L_C2 * (**)	19-09-2014	11-11-2016	27
	L_D2 *	19-09-2014	11-11-2016	27

*one (1) replicate with zinc metal samples; ** Temperature and humidity measurements inside the collector

After approximately two years of exposure (see Exposure time in Table 5), the collectors with zinc samples were tested for thermal performance and dismantled after. Measurement of optical properties was performed in different points of the absorber. These results also presented in this section.

Fig. 6 to 8 show the collector's power curve according to the definition of ISO 9806:2013, comparing the thermal performances after exposure with the initial thermal performance, measured in collectors of the same type before exposure.

In Table 6 the average relative difference between the power curves is presented.

Fig. 6 and 7 show the thermal performance after two years of exposure in Sines and Lumiar-Lisboa OET sites for collectors with aluminum absorbers and PVD coatings (Mirotherm ® and Eta plus ®, respectively) (models A and C). After two years exposure in Sines and Lumiar-Lisboa, collector A does not show significant degradation – average power difference of -0.9% and -1.8%, respectively. Collector model C exposed in Sines shows degradation – average power difference of -6.2%. After two years in Lumiar-Lisboa no significative difference is observed in this collector (model C) – average power difference of -1.1%.

Fig. 8 shows the impact of two years of exposure of collectors with copper absorber and paint coating SUNCOLOR TS S Black (Model D). The collector exposed in Sines shows sixthly lower power curve while in Lumiar-Lisboa the collector exposed after two years shows higher thermal performance – average power difference of +3.0%.

Tab. 6: Average difference of power curve relative to initial peak power (%) in the temperature range 0-90 K

Collector sample	Exposure time (month)	Average difference of power curve relative to initial peak power (%) in the temperature range 0-80 K
S_A2 * (**)	26	-0.9
S_C2 * (**)	25	-6.2
S_D2 *	26	-0,9
L_A2 * (**)	30	-1.8
L_C2 * (**)	27	-1.1
L_D2 *	27	3.0

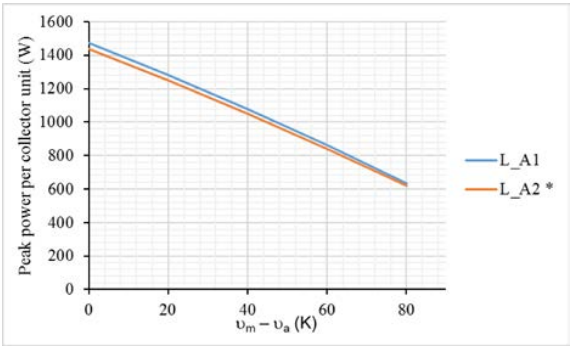

Fig. 6a): Power curves of collector model A (L_A1 – initial measurement: L_A2 * – measurement after two years).

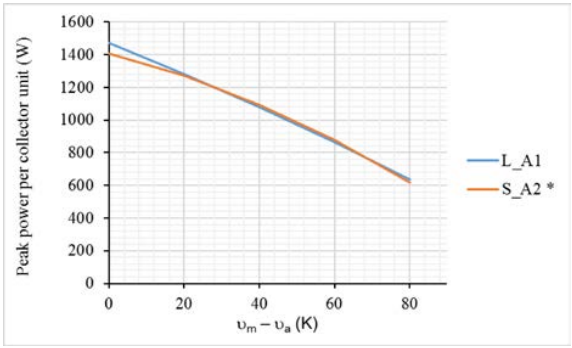

Fig. 6b): Power curves of collector model A (L_A1 – initial measurement: S_A2 * – measurement after two years).

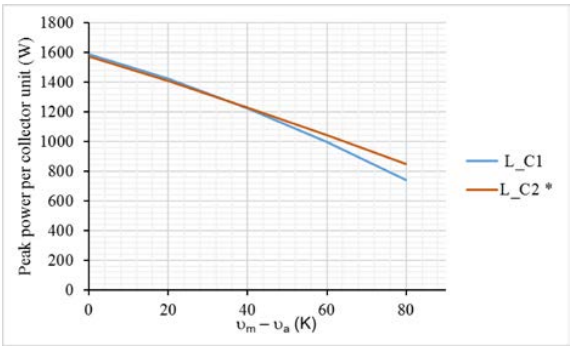

Fig. 7a): Power curves of collector model C (L_C1 – initial measurement: L_C2 * – measurement after two years).

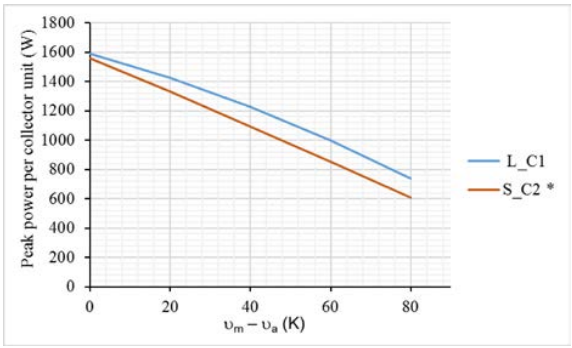

Fig. 7b): Power curves of collector model C (L_C1 – initial measurement: S_C2 * – measurement after two years).

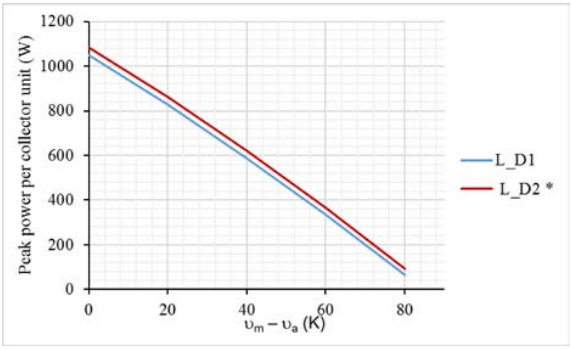

Fig. 8a): Power curves of collector model D (L_D1 – initial measurement: L_D2 * – measurement after two years).

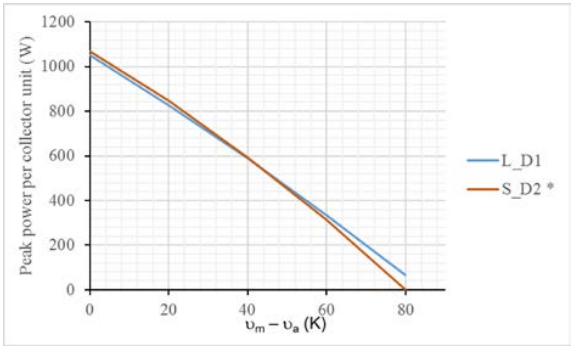

Fig. 8b): Power curves of collector model D (L_D1 – initial measurement: S_D2 * – measurement after two years).

In Table 7 the optical properties of the absorbers of the three collector models are listed. Initial values were obtained from measurement of thirty samples of the absorber used in each collector. The values after two years of exposure were measured in different sections of the collector's absorber after dismantling.

The initial values of the optical properties correspond to average values of thirty samples with corresponding standard deviation. The values after approximately two years correspond to values of measurements made on two or three different samples of the absorber (top, center and bottom) and, when more than one measurement was made, the standard deviation is given.

For collectors A with aluminum substrate and PVD coating, the variation in the solar absorptance is in agreement with the change in peak power (see Fig. 6) for both Sines and Lumiar-Lisboa. The thermal emittance shows a

higher change in Lumiar-Lisboa than in Sines. There are no significant differences between values in the center and bottom of the collector.

For collectors C the solar absorptance does not show significant difference although some change in peak power measured (see Figure 7) is observed. A change in glass transparency may be the reason for this. For Lumiar-Lisboa a higher change in thermal emittance is also observed and this change is not uniform. In Sines, the bottom part of the absorber shows higher thermal emittance values while in Lumiar-Lisboa the center part of the absorber shows higher thermal emittance values.

Tab. 7: Optical properties of collector absorber coatings

Note: Figures in parentheses indicate that the standard deviation observed is lower than the measurement uncertainty.

Collector sample	Exposure time (month)	Location inside collector	α	σ_α	ε	σ_ε
	Initial	**---**	**0.96**	**0.00(1)**	**0.11**	**0.00(2)**
S_A2 *	26	center	0.94	0.00(1)	0.13	0.01
		bottom	0.94	0.00(1)	0.12	0.0(0)
L_A2 *	30	center	0.94	0.00(1)	0.16	0.01(2)
		botom	0.94	0.00(2)	0.15	0.00(9)
	Initial	**---**	**0.96**	**0.00(0)**	**0.11**	**0.00(3)**
S_C2 *	25	center	0.95	--	0.11	--
		bottom	0.95	--	0.14	--
L_C2 *	27	top	0.94	0.00(2)	0.15	0.02
		center	0.94	0.00(2)	0.18	0.02
		bottom	0.94	0.00(2)	0.16	0.01
	Initial	**---**	**0.95**	**0.00(1)**	**0.72**	**0.02**
S_D2 *	26	center	0.93	--	0.56	--
		bottom	0.93	0.00(1)	0.56	0.00(4)
L_D2 *	27	top	0.93	0.00(1)	0.55	0.01
		center	0.93	0.00(1)	0.57	0.01
		bottom	0.93	0.0005	0.58	0.006

3.3. Zinc corrosion rate inside STC and atmospheric contaminants evaluation

Table 8 and 9 present the results of zinc corrosion rate and results of chemical analysis inside the STC in Sines and Lumiar-Lisboa OET site, respectively.

Tab. 8: Zinc corrosion rate and results of chemical analysis inside the STC in Sines OET site.

STC	Position inside collector	Chlorides (mg L^{-1})	Nitrates (mg L^{-1})	Sulfates (mg L^{-1})	Zinc corrosion rate inside collectors r_{corr} (g m^{-2} y^{-1}) (SD)	Corrosion category according to ISO 9223:2012
A	1	0.8	<1	<1	90.31 (9.53)	CX
	2	0.7	<1	<1		
	3	1.7	1.6	<1		
C	1	0.7	<1	<1	99.91 (10.63)	CX
	2	1.0	<1	<1		
	3	4.1	1.8	<1		
D	1	1.5	<1	<1	4.56 (0.55)	C2
	2	1.0	<1	<1		
	3	8.0	2.0	<1		

Tab. 9: Zinc corrosion rate and results of chemical analysis inside the STC in Lumiar-Lisboa OET site.

STC	Position inside collector	Chlorides (mg L^{-1})	Nitrates (mg L^{-1})	Sulfates (mg L^{-1})	Zinc corrosion rate inside collectors r_{corr} (g m^{-2} y^{-1}) (SD)	Corrosion category according to ISO 9223:2012
A	1	<0.5 (QL)	<0.5 (QL)	<0.5 (QL)	47.76 (3.12)	C5
	2	0.74	<0.5 (QL)	<0.5 (QL)		
	3	<0.5 (QL)	<0.5 (QL)	<0.5 (QL)		
C	1	0.5	<0.5 (QL)	<0.5 (QL)	- (*)	-
	2	0.7	<0.5 (QL)	<0.5 (QL)		
	3	1.4	<0.5 (QL)	<0.5 (QL)		
D	1	0.53	<0.5 (QL)	<0.5 (QL)	6.84 (0.24)	C3
	2	1.0	1.0	<0.5 (QL)		
	3	1.1	<0.5	<0.5 (QL)		

(QL) - Quantification limit; (*) It was not possible to evaluate the zinc corrosion rate because the reference materials fell due to the degradation of the polymeric screws that held them.

From the presented results, it is possible to see that the concentration of contaminants is higher at the base of the collectors relative to the top and to the middle. The concentration of contaminants in the absorber surfaces is highest for collector D and lowest for collector A in Sines OET site. The collectors in Sines show higher contaminants concentration than in Lumiar-Lisboa.

It is also possible to see that in Sines, collector D has, for zinc a lower corrosivity than collectors A and C. Between collectors A and C, the corrosivity inside collector C is higher than in collector A. This can be related to the fact that collector C showed a higher concentration of contaminants and reaches higher internal temperatures (Figure 9).

Although temperature and humidity inside collector D was not monitored, its thermal performance clearly indicates that the collector has lower stagnation temperature than collectors A and C. The tightness also seems to be smaller with respect to the collectors A and C.

In Sines the zinc corrosion rate inside the collectors can be associated with the contaminants but the temperature seems to be a determining factor.

The corrosivity inside the collector A is lower in Lumiar-Lisboa than in Sines. However, for the collector D the zinc corrosion rate in Lumiar-Lisboa collector is a little higher than in Sines. Although the concentration of contaminants is lower in Lumiar-Lisboa than in Sines, this may be justified by the fact that a great condensation has been observed in the case of this collector in Lumiar-Lisboa, much higher than in the collector exposed in Sines. Taking into account that zinc reaches in air-saturated water the higher corrosion rate between 60-80ºC (X. G. Zhang, 2011), it can justify the little higher corrosion rate observed in Lumiar-Lisboa. The greater condensation in Lumiar's collector may have contributed more to zinc corrosion than the higher concentration of contaminants in Sines.

3.4. Environmental characterisation of collectors inlet

Figure 9 shows the maximum measured values of temperature in collector models A and C, in Sines and Lumiar-Lisboa, respectively. Figure 10 shows the average measured values of humidity in collector models A and C, in Sines and Lumiar-Lisboa respectively.

The measurement period is different in Sines and Lumiar-Lisboa but it covers in both cases almost one year. In Sines measurements where made between June 2015 to April 2016 and in Lumiar-Lisbooa between December 2014 to October 2015.

The sensors were placed in the upper left or right corner of the collectors.

The measurements show higher temperatures in collector C then in collector A. This is coherent with the relative humidity values that are higher in collector A then in collector C, although results for Lumiar-Lisboa in February and March are not in agreement with this tendency.

On a daily bases the evolution of temperature and relative humidity can be seen in Figure 11.

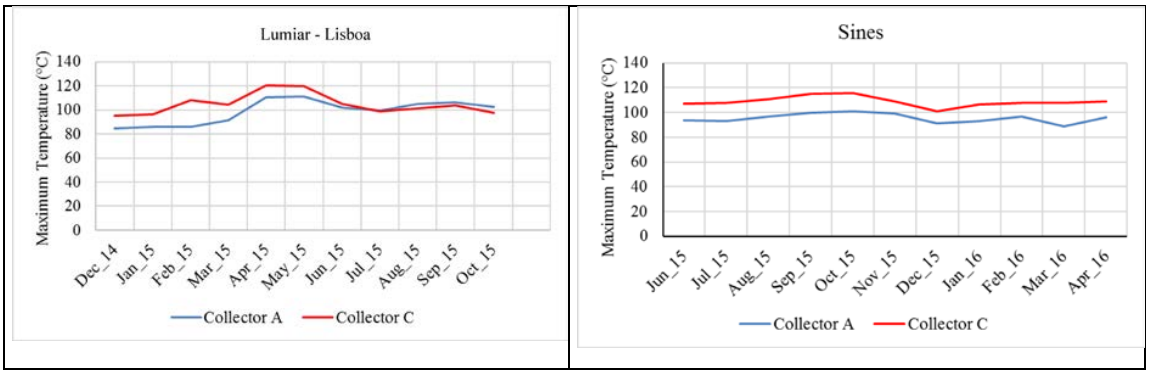

Fig. 9: Maximum measured values of temperature in collector models A and C

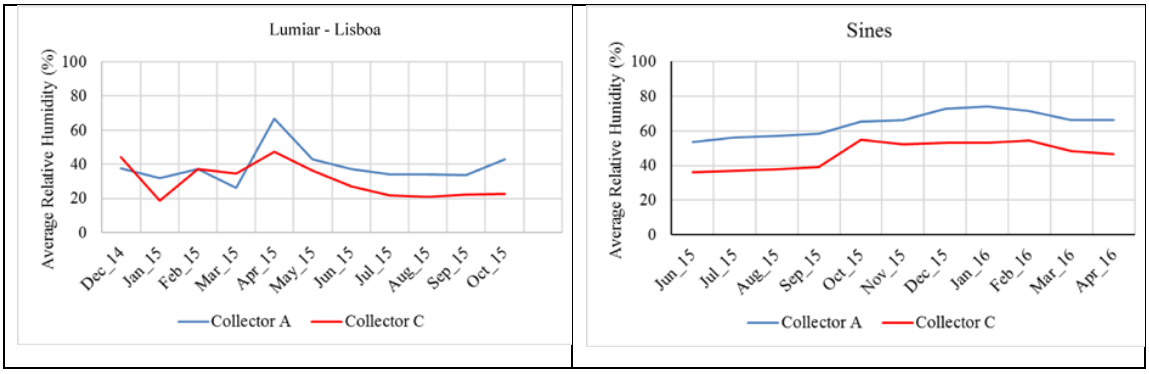

Fig. 10: Average measured values of humidity in collector models A and C

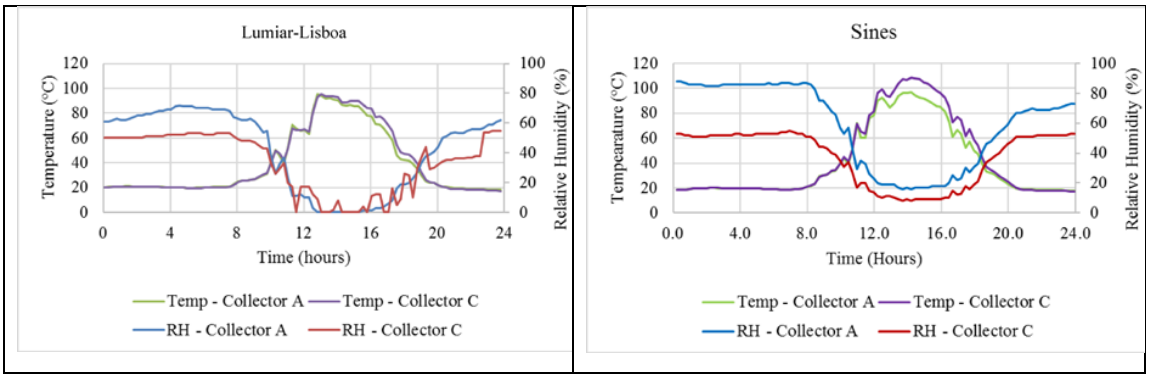

Fig. 11: Representation of one day data (Temperature and relative humidity for collector models A and C) in Lumiar-Lisboa (left) and Sines (right).

3.5. Scanning Electron Microscopy (SEM) with Energy Dispersive X-ray Spectroscopy (EDS)

Table 10 presents SEM micrographs and EDS spectra obtained on solar absorber surfaces inside STC after two years of exposure in Sines OET site.

By SEM was possible to observe the selective surfaces from the three STC and to verified that the surface where there are major changes due to corrosion is on the surface of the collector C, where the chlorine and sulfur elements are present in the corrosion products.

In collector A sodium chloride deposits are observed on the surface but no corrosion products are detected by SEM on the surface.

On the surface of collector D are also visible atmospheric contaminants and some coating cracking / degradation, as well as sodium chloride deposits. Considering that this coating initially had some application defects, it is not possible to distinguish if these observed changes are due to initial corrosion process or to the initial defects of the application.

Tab. 10: SEM micrographs and EDS results of the chemical elements identified on solar absorber surfaces inside STC in Sines OET site after two years

STC	SEM micrographs	EDS spectrum of chemical elements detected
A	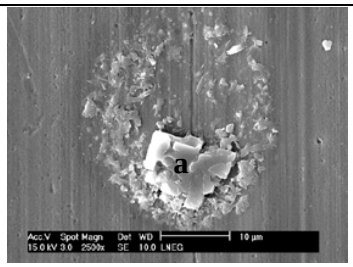	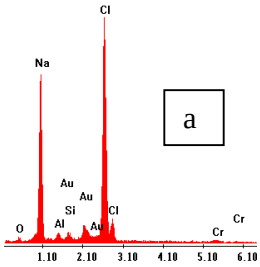
C	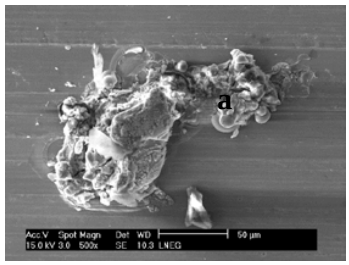	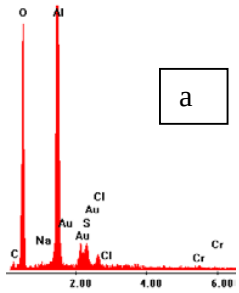
D	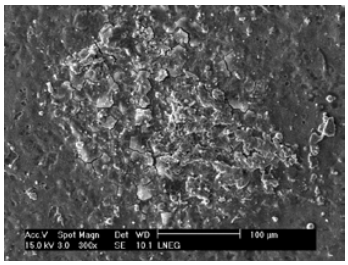	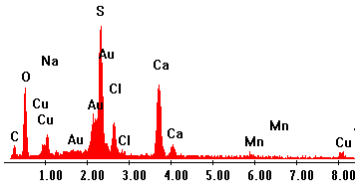

4. Conclusions

After two years exposure, the measurement of thermal performance of the STC shows higher decrease in Sines than in Lumiar-Lisboa for collectors A and C. The decrease in thermal performance is higher for collector C than collector A, especially in Sines. These results are in agreement with higher level of contaminants, especially chlorides, and also in line with the corrosion rates for zinc measured in Sines and Lumiar-Lisboa for collectors A and C.

In the case of collector D, the variation of the thermal performance does not show a clear relation to the location. This may be because the manufacturing process of the collector is not completely controlled. Differences in initial thermal performance of each collector were not detected since the initial measurement was done in only one collector of model D. The low corrosion rates for zinc in this case may be a result of much lower temperature levels in this collector. Although the temperature and humidity was not monitored in this case, the thermal performance of the collector indicates a lower stagnation temperature than in collectors A and C.

The contaminants present on the different solar absorber surfaces were also different depending on the type of collector. Different ventilation rates and higher temperatures in collectors A and C may explain these differences in terms of contaminants and zinc corrosion rate.

The contaminants detected on the absorbers are mainly chlorides in all collectors and nitrates (Sines OET). The concentration of sulfates and nitrates are low and in some cases below the limits of quantification. From the observations by SEM made for the absorbers of collectors exposed in Sines, we may correlate changes due to

corrosion in collector C to the presence of contaminants. In the case of collector A, although chlorine was present on the surface, no corrosion was observed. The high corrosion resistance of PVD present in collector A relatively to collector C is in agreement with the results presented for these selective surfaces exposed in OET sites (Diamantino et al. 2017) and in accelerated aging tests (Diamantino et al, 2016).

Two years exposure is still a short period to correlate thermal performance decrease with corrosion due to atmospheric contaminants but it is possible to identify the importance of chloride for locations like Sines and the need to introduce this contaminant in the accelerated aging tests for qualification of absorber surfaces. ISO 22975-3:2014 only considers sulfur as contaminant.

5. Acknowledgements

This work is a result of the project FCOMP-01-0124-FEDER-027507 (Refª FCT RECI/EMS-ENE/0170/2012) supported by Operational Competitiveness Programme (COMPETE) through the European Regional Development Fund (ERDF) and supported by FCT- Fundação para a Ciência e a Tecnologia, I.P. through National Funds and the project POCI-01-0145-FEDER-016709 (Refª FCT PTDC/EMS-ENE/0578/2014) supported by COMPETE 2020 and LISBOA 2020 under the PORTUGAL 2020 Partnership Agreement through the European Regional Development Fund (ERDF) and supported by FCT through National Funds.

The authors would like to thank to industrial partners (FogãoSol, Hempel, OpenPlus and Permasolaris), by the supply of samples and the means for performing this work.

6. References

Carvalho, M. J., Páscoa, S., Gonçalves, R., Mexa, N., Diamantino, T. C., 2016, Influence of maritime/industrial atmosphere on solar thermal collector's degradation, Comunication to Eurosun 2016, Palma de Maiorca, Spain doi:10.18086/eurosun.2016.07.04 (http://proceedings.ises.org/?mode=list&conference=eurosun2016)

Diamantino, T. C., Gonçalves, R., Nunes, A., Páscoa, S., Carvalho, M. J., 2017. Durability of different selective solar absorber coatings in environments with different corrosivity. Solar Energy Materials & Solar Cells Vol. 166, July 2017, Pages 27–38 (http://dx.doi.org/10.1016/j.solmat.2017.03.004)

Diamantino, T. C., A. Nunes, R. Gonçalves, S. Páscoa, T. Chambino and M. J. Carvalho., 2016 Selective Absorber Coatings Qualification - ISO 22975-3:2014. Full Application. Comunication to Eurosun 2016, Palma de Maiorca, Spain. doi:10.18086/eurosun.2016.06.01 (http://proceedings.ises.org/?mode=list&conference=eurosun2016)

Köhl, M., B. Carlsson, G.J. Jorgensen, A.W. Czanderna (Eds.), Performance and Durability Assessment. Optical Materials for Solar Thermal Systems, Elsevier, Oxford, 2004.

ISO 8502-6:2006 Preparation of steel substrates before application of paints and related products. Tests for assessment of surface cleanliness. Part 6: Extraction of soluble contaminants for analysis. The Bresle method

ISO 9223:2012 Corrosion of metals and alloys - Corrosivity of atmospheres - Classification, determination and estimation. 2012

ISO 9226:2012 Corrosion of metals and alloys - Corrosivity of atmospheres - Determination of corrosion rate of standard specimens for the evaluation of corrosivity. 2012

ISO 9806:2013(E), Solar Energy – Solar Thermal Collectors – Test Methods

ISO 22975-3:2014 Solar energy -- Collector components and materials -- Part 3: Absorber surface durability, 2014

Slamova, K., Duerr, I., Kaltenbach, T., Köhl, M., 2016. Degradation effects of maritime atmosphere on metallic components of solar collectors. Solar Energy Materials & Solar Cells 147, 246–254 (http://dx.doi.org/10.1016/j.solmat.2015.12.011)

Zhang, X. G., Uhlig's Corrosion Handbook, R. Winston Revie (editor). 3rd Edition; New Jersey: Wiley, (2011) (pp879-892) ISBN: 978-0-470-08032-0,